

Asymptotic Analysis of MIMO Channels With Transmitter Noise and Mismatched Decoding

Mikko Vehkaperä, Taneli Riihonen, Maksym Girnyk, Emil Björnson,
Mérrouane Debbah, Lars K. Rasmussen, and Risto Wichman

Abstract—Hardware impairments in radio-frequency components of a wireless system cause unavoidable distortions to transmission that are not captured by the conventional linear channel model. In this paper, a ‘binoisy’ multiple-input multiple-output (MIMO) relation is considered where the additional distortions are modeled via an additive noise term at the transmit side. Through this extended MIMO channel model, the effects of transceiver hardware impairments on the achievable rate of multi-antenna point-to-point systems are studied. General channel input distributions encompassing all conventional digital modulation schemes as well as Gaussian signaling are covered. In addition, the impact of mismatched detection and decoding when the receiver has insufficient information about the non-idealities is investigated. The numerical results show that for realistic system parameters, the effects of transmit-side noise and mismatched decoding become significant only at high modulation orders.

I. INTRODUCTION

MIMO, i.e., multiple-input multiple-output, wireless links are a mature research subject and their theory is already well understood [1]. However, the extensive body of literature on link-level analysis conventionally concerns signal models of the form $\mathbf{y} = \mathbf{H}\mathbf{x} + \mathbf{n}$ reckoning with an additive thermal-noise term, namely \mathbf{n} , only at the receiver after the fading channel \mathbf{H} . In this paper, we adopt a generalized (‘binoisy’) input–output relation from [2]–[11]:

$$\mathbf{y} = \mathbf{H}(\mathbf{x} + \mathbf{v}) + \mathbf{w}, \quad (1)$$

where \mathbf{w} is an additive receive-side distortion-plus-noise component. The system model (1) allows including an additive noise term, namely \mathbf{v} , also at the transmitter, thus making the total effective noise term $\mathbf{H}\mathbf{v} + \mathbf{w}$ colored and correlated with the fading channel. This small but significant complement yields a MIMO link model whose performance analysis is still an open research niche in many respects.

Although we primarily aim at extending the capacity theory of binoisy MIMO channels under fading without committing to any particular application, the signal model (1) originally stems from the practical need for modeling various transceiver hardware impairments which are detailed in [12], [13], and the references therein. However, it is worth to acknowledge that additive noise is only a simplified representation of complex nonlinear phenomena occurring due to hardware impairments, especially when considering their joint coupled effects or trying to model residual distortion after compensation. Thus, the binoisy signal model should be regarded as a compromise

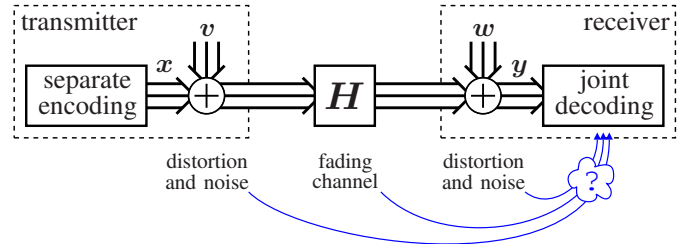


Fig. 1. System model for non-ideal MIMO communications with transmit and receive distortion. The receiver might be misinformed or ignorant of some of the variables in the transmission chain leading to mismatched decoding.

between facilitating theoretical analysis and resorting to measurements or simulations under more accurate modeling.

Additive receiver hardware impairments can be incorporated into the conventional signal model by increasing the level of the thermal-noise term \mathbf{n} by a constant noise figure, e.g., about 3–5 dB, or by scaling it in proportion to the input signal level such that it matches with \mathbf{w} . On the other hand, regarding the joint effect of transmitter hardware impairments as an additive transmit-side noise term \mathbf{v} is analogous to the principles of practical radio conformance testing. In particular, the common transmitter quality indicator is error-vector magnitude (EVM) which reduces the distortion effects to an additive component and measures its level relatively to signal amplitude [14].

Typical target EVM values guarantee that the signal \mathbf{x} is at least 20–30 dB above the transmit-side noise \mathbf{v} . On the other hand, for basic discrete channel inputs such as quadrature phase-shift keying (QPSK), $\mathbf{H}\mathbf{x}$ is usually at most 10–15 dB above the receive-side noise \mathbf{w} , after which the communication is not anymore limited by noise but the lack of entropy in the modulation alphabet. This implies that transmitter hardware impairments can be justifiably omitted in the analysis of simple low-rate wireless systems: Either $\mathbf{H}\mathbf{v}$ is well below the receive-side noise \mathbf{w} (say 5–20 dB) or the signal-to-noise ratio (SNR) is set to an uninterestingly high level. However, there has been a trend to improve data rates by using, e.g., quadrature amplitude modulation (QAM) up to 64-QAM at relatively high SNR, in which case the transmit-side noise begins to play a notable role in the link-level performance.

The considered system setup corresponding to (1) is shown in Fig. 1. As for MIMO processing, we focus on regular spatial multiplexing where a conventional transmitter separately encodes and sends an independent stream at each of its antennas without having channel state information or being aware of the transmit-side noise it produces; the receiver jointly decodes the output signals of the MIMO channel knowing its instantaneous

realization \mathbf{H} and some noise statistics. However, conventional receivers are designed and implemented based on the conventional signal model (where $\mathbf{v} = \mathbf{0}$) due to which they are prone to lapse into suboptimal *mismatched decoding* by inaccurately postulating the statistics of the actual noise term $\mathbf{H}\mathbf{v} + \mathbf{w}$. Even if off-the-shelf receivers can adapt to colored receiver noise, they may not be able to track the variable statistics of the component $\mathbf{H}\mathbf{v}$ propagated from the transmitter since it is correlated with the fading channel. Only an advanced receiver would be able to perform *matched decoding* knowing perfectly the noise statistics as if it was designed and implemented explicitly based on the generalized binoisy signal model (1).

A. Related Works

The key reference results for the present study are reported in [2]–[11]. These seminal works originally formulated the research niche around (1) and established the baseline understanding of MIMO communication in the presence of transmit-side noise with numerical simulations and theoretical analysis. The majority of the related works, e.g., [2], [3], [6], [8], concern regular spatial multiplexing using separate encoding like the present paper but also different variations of joint encoding have been creditably investigated, e.g., in [4], [7]. On the other hand, all the studies that we are aware of assume (implicitly) advanced receivers that know the presence of transmit noise, no matter what form of decoding is used.

Especially, the reference results are polarized such that the scope of analytical studies [6], [8] typically differs from that of studies reporting simulations [6], [7], [9] or measurements [4]–[6]. Except for [2], practical discrete modulation schemes, e.g., QAM, have not been previously analytically evaluated in the presence of transmit noise, and simulation-based studies usually concern bit/symbol/packet error rates, not transmission rates which could be more interesting when studying modern adaptive encoding. In contrast, all the analytical capacity studies assume Gaussian signaling and the throughput simulations of [3] with adaptive modulation and coding are their closest counterpart when it comes to experimental work.

If the receiver does not properly account for the additional transmit-side noise in the received signal, conventional mutual information (MI) is not anymore the correct upper bound for coded transmissions. Rather, due to mismatched decoding, one has to employ other metrics, such as *generalized mutual information* (GMI) [15], [16] adopted herein. Another common use for GMI is the analysis of bit-interleaved coded modulation [17], while also transceiver hardware impairments [18] and effects of imperfect channel state information at multi-antenna receiver [19] are analyzed in terms of GMI. In particular, MI and GMI are evaluated herein using the *replica method* [20], originating from the field of statistical physics and introduced to the analysis of wireless systems by [21], [22]. Since then, the replica method has been applied to various problems in communication theory, e.g., MIMO systems [23]–[25]. For some special cases like Gaussian signaling, the replica trick renders exact asymptotic results when the number of antennas grows without bound, while they can be otherwise considered accurate approximations as shown by comparisons to Monte Carlo simulations.

B. Summary of Contributions

In this paper, we investigate two aspects of binoisy MIMO channels that are unexplored in related works despite their fundamental role in understanding the effects of hardware impairments in wireless systems. Firstly, analytical capacity results are limited to Gaussian signaling while practical digital modulation is evaluated only based on simulations or measurements. Secondly, the earlier literature focuses on the optimistic case of matched decoding by employing receivers that are actually not available off the shelf but implicitly updated to take account of transmit-side noise.

In particular, this paper contributes to the capacity theory of MIMO communication links by examining the effects of transmit-side noise as follows.

- Analytical GMI expressions are calculated for studying the rate loss of mismatched decoding when using a conventional receiver which is unaware of the transmit-side noise. Especially, it is shown that the performance remains the same irrespective of how well the noise covariance matrix is known if it is a constant.
- The above analysis is further translated into corresponding asymptotic high-SNR limits for Gaussian signaling as a complement for the results of [10], which covers matched decoding and conventional MI.
- The analytical expressions provided for both conventional MI and GMI cover all practical discrete modulation schemes such as the variations of PSK and QAM. They can be also used for corroborating the existing results available for Gaussian signaling.

Extending beyond the scope of the paper, the replica analysis of GMI is also a new aspect at large.

C. Outline of the Paper and Its Nomenclature

After the considered system model is specified in the following section, the main analytical content of this paper is divided into two parts: Section III concerns the performance of conventional suboptimal receivers under mismatched decoding, which is analyzed based on GMI; and Section IV studies conventional MI with advanced receivers, which are aware of transmitter noise and, thus, capable of optimal matched decoding. In Section V, the presented theory is illustrated with numerical results, including simulations for double-checking its accuracy, which is finally followed by concluding remarks in the last section. Appendix A summarizes some general results that are used throughout the paper while Appendices B and C contain the derivations of the main results.

Notation: Complex Gaussian random variables (RVs) are always assumed to be proper and the density of such $\mathbf{x} \in \mathbb{C}^N$ with mean $\boldsymbol{\mu}$ and covariance \mathbf{R} is denoted $g(\mathbf{x} | \boldsymbol{\mu}; \mathbf{R})$. For the zero-mean proper Gaussians, we say they are circularly symmetric complex Gaussian (CSCG). For convenience, both discrete and continuous RVs are said to have a probability density function (PDF) that is denoted by p , and we do not separate RVs and their realizations. For postulated PDFs we write q and add tilde on top of the related RVs (most of the time). Given a RV x that has a PDF $p(x)$, we write $x \sim p(x)$ (and $\tilde{x} \sim q(\tilde{x})$ for the postulated case). Statistical expectation

is denoted $E\{\cdot\}$ and is with respect to (w.r.t.) true or postulated PDFs, depending on the arguments. Integrals w.r.t. real-valued variables are always over \mathbb{R} (for vectors over the appropriate product space) and we tend to omit the integration limits for notational simplicity. For a complex variable $z = x + jy$, we denote $\int(\cdot)dz = \int(\cdot)dx dy$, and similarly for complex vectors. Logarithms are natural logs and denoted \ln unless stated otherwise.

II. SYSTEM MODEL

Consider the system model depicted in Fig. 1 and the signal model of $\mathbf{y} \in \mathbb{C}^N$ written in (1) where $\mathbf{H} \in \mathbb{C}^{N \times M}$ is the channel matrix and $\mathbf{x} \in \mathbb{C}^M$ the signal of interest. The receive-side distortion plus noise component is divided into two parts, namely $\mathbf{w} = \mathbf{n} + \boldsymbol{\omega} \in \mathbb{C}^N$ where \mathbf{n} is caused by thermal noise and $\boldsymbol{\omega}$ represents hardware impairments arising from the non-ideal behavior of the radio-frequency (RF) transceivers. Similarly, $\mathbf{v} = \mathbf{m} + \boldsymbol{\nu} \in \mathbb{C}^M$ where \mathbf{m} and $\boldsymbol{\nu}$ are related to thermal noise and hardware impairments or distortions, respectively, at the transmit-side. In practice, the effect of \mathbf{m} is often negligible compared to $\boldsymbol{\nu}$. In conventional MIMO literature it is common to consider only the thermal noise at the receiver, which translates to assuming $\boldsymbol{\omega} = \boldsymbol{\nu} = \mathbf{m} = \mathbf{0}$ in our more generic system model.

Let us denote the PDF of the transmit vector \mathbf{x} by $p(\mathbf{x})$ and assume it factorizes as

$$p(\mathbf{x}) = \prod_{m=1}^M p(x_m), \quad (2)$$

so that independent streams are transmitted at each transmit antenna. Furthermore, let $p(x_m)$ be a zero-mean distribution with variance $\bar{\gamma}_m$. For later convenience, we let $\mathbf{\Gamma}$ be a diagonal matrix whose non-zero elements are given by $\bar{\gamma}_1, \dots, \bar{\gamma}_M$, that is, $\mathbf{\Gamma} = E\{\mathbf{x}\mathbf{x}^H\}$. The channel \mathbf{H} is assumed to have independent identically distributed (IID) CSCG elements with variance¹ $1/M$. The thermal noise samples at the transceivers are modeled as CSCG random vectors \mathbf{m} and \mathbf{n} that have independent elements. For simplicity, we assume that any given noise or hardware impairment component is independent of any other RVs in the system. The transmit- and receive-side impairments $\boldsymbol{\nu}$ and $\boldsymbol{\omega}$ are taken to be CSCG random vectors with covariance matrices \mathbf{R}_ν and \mathbf{R}_ω , respectively. The distortion plus noise vectors \mathbf{v} and \mathbf{w} are thus CSCG random vectors whose covariance matrices we denote \mathbf{R}_v and \mathbf{R}_w , respectively. Notice that these matrices can be functions of the statistics of some other RVs albeit we suppress the explicit statement of such dependence at this point for notational convenience. The SNR without transmit-side noise is defined as $\text{tr}(\mathbf{\Gamma})/\text{tr}(\mathbf{R}_w)$.

¹Common assumption in MIMO systems is that the total power emitted from the transmit antennas is constant; that is, $\text{tr}(\mathbf{\Gamma}) = \bar{\gamma}$, where $\bar{\gamma}$ is some fixed power budget that does not depend on M . Hence the elements of $\mathbf{\Gamma}$ need to be functions of M in order to satisfy the transmit power normalization. For the following analysis, however, it is more convenient to treat the elements of $\mathbf{\Gamma}$ to be independent of M and let the transmit power normalization be a part of the channel. Clearly, both approaches are mathematically fully equivalent.

The PDF of the received signal, conditioned on \mathbf{x} , \mathbf{v} and \mathbf{H} , is given by

$$p(\mathbf{y} | \mathbf{x}, \mathbf{v}, \mathbf{H}) = g(\mathbf{y} | \mathbf{H}(\mathbf{x} + \mathbf{v}); \mathbf{R}_w), \quad (3)$$

and the receiver is assumed to know \mathbf{H} and the true distribution $p(\mathbf{x})$ of the channel input. However, the additional transmit-side term \mathbf{v} is in general unknown at the receive-side and, thus, the PDF (3) cannot be directly used for detection and decoding. Herein, we consider two different scenarios for the joint decoding operation at the receiver:

- 1) The receiver knows \mathbf{H} , the PDFs of the noise plus distortion terms \mathbf{v} and \mathbf{w} as well as the distribution of the data vector \mathbf{x} . *Matched joint decoding* is then based on the conditional PDF

$$p(\mathbf{y} | \mathbf{x}, \mathbf{H}) = E_v\{g(\mathbf{y} | \mathbf{H}(\mathbf{x} + \mathbf{v}); \mathbf{R}_w)\} \quad (4)$$

$$= g(\mathbf{y} | \mathbf{H}\mathbf{x}; \mathbf{R}_w + \mathbf{H}\mathbf{R}_v\mathbf{H}), \quad (5)$$

where the second equality follows from (60)–(62) in Appendix A. Note that the effective noise covariance matrix in (5) depends now on the instantaneous channel realization \mathbf{H} .

- 2) The receiver has perfect knowledge of \mathbf{H} and the PDF of the data vector \mathbf{x} . Instead of (4), however, the device uses a postulated channel law

$$q(\mathbf{y} | \mathbf{x}, \mathbf{H}) = g(\mathbf{y} | \mathbf{H}\mathbf{x}; \tilde{\mathbf{R}}), \quad (6)$$

for *mismatched joint decoding*. In contrast to (5), the postulated covariance matrix $\tilde{\mathbf{R}}$ is fixed and independent of the realizations of any other RV in the system.

If matched joint decoding is employed, the conventional metric for evaluating the (ergodic) achievable rate of the system for given input distribution $p(\mathbf{x})$ is the MI between the channel inputs and outputs, namely,

$$I(\mathbf{y}; \mathbf{x}) = E\{\ln p(\mathbf{y} | \mathbf{x}, \mathbf{H})\} - E\{\ln p(\mathbf{y} | \mathbf{H})\}, \quad (7)$$

where $p(\mathbf{y} | \mathbf{H}) = E_{\mathbf{x}}\{p(\mathbf{y} | \mathbf{x}, \mathbf{H})\}$. From the system design perspective, however, it might be impractical to use (5) due to complexity of implementation, resulting in mismatched decoding. To lower bound the true maximum rate that can be achieved reliably over channel (1) when decoding rule (6) is used at the receiver, we use GMI that is discussed in the next section.

III. MISMATCHED JOINT DECODING: GENERALIZED MUTUAL INFORMATION

A. Definition and the Special Case of Gaussian Signaling

Let us assume that the received signal is given by (1) but the receiver uses (6) for joint decoding. Given $p(\mathbf{x})$, the (ergodic) GMI between the channel inputs and outputs is defined as [15], [16]

$$I_{\text{GMI}}(\mathbf{y}; \mathbf{x}) = \sup_{s>0} I_{\text{GMI}}^{(s)}(\mathbf{y}; \mathbf{x}), \quad (8)$$

where, denoting $q^{(s)}(\mathbf{y} | \mathbf{H}) = E_{\mathbf{x}}\{q(\mathbf{y} | \mathbf{x}, \mathbf{H})^s\}$, the s -dependent part reads

$$I_{\text{GMI}}^{(s)}(\mathbf{y}; \mathbf{x}) = E\{\ln q(\mathbf{y} | \mathbf{x}, \mathbf{H})^s\} - E\{\ln q^{(s)}(\mathbf{y} | \mathbf{H})\}. \quad (9)$$

If I is the maximum ergodic rate that can be transmitted over the channel (1) using input distribution $p(\mathbf{x})$ and decoding rule (6), then $I \geq I_{\text{GMI}}$ [15], [16]. In this paper, the decoding based on the true channel law (4) cannot be obtained as a special case of the mismatched case since $\tilde{\mathbf{R}}$ is fixed (cf. Appendix B). Therefore, the case of matched decoding is considered separately in Section IV.

We are first interested in evaluating the s -dependent part of the normalized GMI per transmit stream $M^{-1}I_{\text{GMI}}^{(s)}(\mathbf{y}; \mathbf{x})$ for given $s > 0$. The optimization over the free parameter s is carried out after the suitable expressions are found. The first term in (9) can be written as

$$\begin{aligned} & \frac{1}{M} \mathbb{E} \{ \ln q(\mathbf{y} | \mathbf{x}, \mathbf{H})^s \} \\ & = - \frac{s}{M} \left[N \ln \pi + \ln \det \tilde{\mathbf{R}} \right] \\ & \quad - \frac{s}{M} \mathbb{E} \{ (\mathbf{H}\mathbf{v} + \mathbf{w})^H \tilde{\mathbf{R}}^{-1} (\mathbf{H}\mathbf{v} + \mathbf{w}) \} \\ & = -c^{(s)} - \frac{s}{M} \left[\text{tr}(\tilde{\mathbf{R}}^{-1} \mathbf{R}_w) + \frac{1}{M} \text{tr}(\tilde{\mathbf{R}}^{-1}) \text{tr}(\mathbf{R}_v) \right]. \end{aligned} \quad (10)$$

The first equality follows from (6) by the fact that $\mathbf{y} - \mathbf{H}\mathbf{x} = \mathbf{H}\mathbf{v} + \mathbf{w}$ when \mathbf{x} is given. The second equality is a consequence of the assumption that the channels and noise vectors are all mutually independent and \mathbf{H} has zero-mean IID entries with variance $1/M$. Notice that (10) is independent of $p(\mathbf{x})$ and hence valid for all channel inputs. Evaluating the second term in (9) is more complicated but *for the special case of Gaussian inputs* we have the result shown below.

Example 1. Consider the special case of Gaussian inputs; that is, $p(\mathbf{x}) = g(\mathbf{x} | \mathbf{0}; \mathbf{\Gamma})$. Then,

$$\begin{aligned} \frac{1}{M} I_{\text{GMI}}^{(s)}(\mathbf{y}; \mathbf{x}) &= \frac{1}{M} \mathbb{E}_{\mathbf{H}} \left\{ \ln \det (\tilde{\mathbf{R}} + s \mathbf{H} \mathbf{\Gamma} \mathbf{H}^H) \right. \\ & \quad + s \text{tr} \left[(\mathbf{R}_w + \mathbf{H}(\mathbf{R}_v + \mathbf{\Gamma})\mathbf{H}^H) (\tilde{\mathbf{R}} + s \mathbf{H} \mathbf{\Gamma} \mathbf{H}^H)^{-1} \right] \\ & \quad \left. - s \text{tr}(\tilde{\mathbf{R}}^{-1} \mathbf{R}_w) - \frac{s}{M} \text{tr}(\tilde{\mathbf{R}}^{-1}) \text{tr}(\mathbf{R}_v) - \ln \det \tilde{\mathbf{R}} \right\}, \end{aligned} \quad (11)$$

where we used the identities in Appendix A to obtain (11). \diamond

Example 1 shows that for Gaussian signals we only need to average over the channel to obtain the s -dependent part of GMI. This is quite doable with a straightforward Monte Carlo simulation. It should be remarked, however, that finding the optimal s is time consuming even in this case. Thus, a simple analytical expression that does not explicitly depend on the form of the marginals in (2) would be highly desirable. With this in mind, we impose the following restriction on our system model to simplify the analysis.

Assumption 1. The covariance matrix for the transmit-side distortion plus noise term \mathbf{v} is diagonal so that we may write $\mathbf{R}_v = \mathbf{R}_m + \mathbf{R}_\nu = \text{diag}(r_v^{(1)}, \dots, r_v^{(M)})$. Hence, \mathbf{v} has independent (but not necessarily identically distributed) entries drawn according to $p(v_m) = g(v_m | 0; r_v^{(m)})$.

Finally, we remark that the above assumption is not necessary for the replica analysis but helps to simplify the end result to a form whose numerical evaluation is easy.

B. Analytical Results via the Replica Method

If the goal is to calculate the expectations related to the latter term in (9) analytically and for general input distributions, we need to employ somewhat more advanced analytical tools than the basic probability calculus used in Example 1. As we shall see shortly, employing the replica method provides a formula that is applicable to a variety of input constellations, such as Gaussian or QAM. To begin, let us first denote

$$-\frac{1}{M} \mathbb{E} \ln q^{(s)}(\mathbf{y} | \mathbf{H}) = c^{(s)} + f(s), \quad (12)$$

where $c^{(s)}$ is defined in (10) and the latter term, equivalent of the so-called *free energy* in statistical physics, reads

$$\begin{aligned} & f(s) \\ & = -\frac{1}{M} \mathbb{E} \left\{ \ln \mathbb{E}_{\tilde{\mathbf{x}}} \left\{ e^{-[\mathbf{H}(\mathbf{x} + \mathbf{v} - \tilde{\mathbf{x}}) + \mathbf{w}]^H s \tilde{\mathbf{R}}^{-1} [\mathbf{H}(\mathbf{x} + \mathbf{v} - \tilde{\mathbf{x}}) + \mathbf{w}]} \right\} \right\}. \end{aligned} \quad (13)$$

Notice that the inner expectation over the postulated channel input $\tilde{\mathbf{x}}$ is w.r.t. a generic PDF given in (2) and cannot be solved using (60) in Appendix A. The outer expectation is w.r.t. the rest of the randomness in the system, namely $\{\mathbf{x}, \mathbf{v}, \mathbf{w}, \mathbf{H}\}$. Due to (9) and (10) the expression to be optimized in the GMI formula thus becomes

$$\begin{aligned} & \frac{1}{M} I_{\text{GMI}}^{(s)}(\mathbf{y}; \mathbf{x}) \\ & = f(s) - \frac{s}{M} \left[\text{tr}(\tilde{\mathbf{R}}^{-1} \mathbf{R}_w) + \frac{1}{M} \text{tr}(\tilde{\mathbf{R}}^{-1}) \text{tr}(\mathbf{R}_v) \right]. \end{aligned} \quad (14)$$

Remark 1. By (13) and (14), it is clear that if the receiver assumes that the additive noise in the system is spatially white $\tilde{\mathbf{R}} = \tilde{r} \mathbf{I}_N$ with some finite sample variance \tilde{r} , the GMI remains the same for all $\tilde{r} > 0$ since the optimization over $s > 0$ in (8) can be replaced by an optimization over a new variable $\tilde{s} = s/\tilde{r} > 0$. Thus, if the receiver uses $\tilde{\mathbf{R}} = \tilde{r} \mathbf{I}_N$ for decoding, the GMI is the same for all $\tilde{r} > 0$ when the transmit and receive covariance matrices \mathbf{R}_v and \mathbf{R}_w are fixed. \diamond

The main obstacle in evaluating (14) is $f(s)$ defined in (13). However, this term happens to be of a form that can be tackled by the replica method. The following result is derived in Appendix B under the assumption of the so-called *replica symmetric* (RS) ansatz. Furthermore, the system is assumed to approach the large system limit (LSL), that is, $M, N \rightarrow \infty$ with finite and fixed ratio $\alpha = M/N > 0$. The limit notation is omitted below and the results should therefore be interpreted as approximations for systems that have finite dimensions.

Proposition 1. Let $m = 1, \dots, M$ and denote

$$\chi_m = x_m + v_m, \quad (15)$$

$$\tilde{\chi}_m = \tilde{x}_m, \quad (16)$$

where $x_m, \tilde{x}_m \sim p(x_m)$ and $v_m \sim g(v_m | 0; r_v^{(m)})$ are independent for all m by assumption. Let

$$p(z_m | \chi_m) = g(z_m | \chi_m; \eta^{-1}), \quad (17)$$

$$q(z_m | \tilde{\chi}_m) = g(z_m | \tilde{\chi}_m; \xi^{-1}), \quad (18)$$

be the conditional PDFs of two channels whose inputs (15) and (16) are corrupted by additive white Gaussian noise

(AWGN) with variances η^{-1} and ξ^{-1} , respectively. The parameters η, ξ satisfy the conditions

$$\eta = \frac{1}{\alpha} \frac{\left[\frac{1}{N} \text{tr}(\tilde{\Omega}^{-1}) \right]^2}{\frac{1}{N} \text{tr}(\tilde{\Omega}^{-1} \Omega \tilde{\Omega}^{-1})}, \quad (19)$$

$$\xi = \frac{1}{\alpha N} \text{tr}(\tilde{\Omega}^{-1}), \quad (20)$$

for the given matrices

$$\Omega = \mathbf{R}_w + \varepsilon \mathbf{I}_N, \quad (21)$$

$$\tilde{\Omega} = s^{-1} \tilde{\mathbf{R}} + \tilde{\varepsilon} \mathbf{I}_N, \quad (22)$$

and variables

$$\varepsilon = \frac{1}{M} \sum_{m=1}^M \mathbb{E} \{ |v_m + x_m - \langle \tilde{x}_m \rangle_q|^2 \}, \quad (23)$$

$$\tilde{\varepsilon} = \frac{1}{M} \sum_{m=1}^M \mathbb{E} \{ |\tilde{x}_m - \langle \tilde{x}_m \rangle_q|^2 \}. \quad (24)$$

The notation $\langle \tilde{x}_m \rangle_q$ above refers to a decoupled posterior mean estimator

$$\langle \tilde{x}_m \rangle_q = \frac{\mathbb{E}_{\tilde{x}_m} \{ \tilde{x}_m q(z_m | \tilde{x}_m) \}}{q(z_m)}, \quad (25)$$

where $q(z_m) = \mathbb{E}_{\tilde{x}_m} \{ q(z_m | \tilde{x}_m) \}$. If we also write $p(z_m) = \mathbb{E}_{\chi_m} \{ p(z_m | \chi_m) \}$, the free energy $f(s)$ defined in (14) is given under the assumption of the RS ansatz by

$$\begin{aligned} f_{\text{RS}}(s) &= \frac{1}{\alpha N} \left[\ln \det \tilde{\Omega} + \text{tr}(\tilde{\Omega}^{-1} \Omega) - \ln \det(s^{-1} \tilde{\mathbf{R}}) \right] \\ &\quad - \left(\ln \frac{\pi}{\xi} + \frac{\xi}{\eta} + \frac{1}{M} \sum_{m=1}^M \int p(z_m) \ln q(z_m) dz_m \right) \\ &\quad - \xi \varepsilon + \frac{\xi(\xi - \eta)}{\eta} \tilde{\varepsilon}. \end{aligned} \quad (26)$$

If multiple solutions to the coupled fixed point equations (19) – (24) are found, the one minimizing (26) should be chosen.

Proof: An outline of the derivation is given in Appendix B. ■

The above result extends some previous works such as [21], [22] in the direction of correlated noise at the receiver and additive transmit-side impairments. It is thus clear that the original GMI term (9) of the MIMO system that suffers from transceiver hardware impairments has an interpretation in terms of an equivalent *decoupled*² scalar system. This decoupled channel has only additive distortions but unlike in the conventional case of replica analysis [21], [22], the transmit-side has its own noise term. It should be remarked, however, that the implicit assumption here is that $f_{\text{RS}}(s) = f(s)$; that is, the system is not replica symmetry breaking (RSB). We leave the RSB case as a possible future work and check the validity of the solution with selected numerical simulations.

For simplicity of presentation, we consider next a few practical special cases of Proposition 1 where the transmit power is the same for all antennas and the noise and distortions at

²This decoupling property is ubiquitous in replica analysis, see for example [21], [22], and is one of the key reasons why the replica method provides computationally feasible solutions for complex problems.

TABLE I
HOW TO OBTAIN GMI FOR GAUSSIAN SIGNALING FROM EXAMPLE 2

- 1) Choose the parameters that define the MIMO system of interest, namely, antenna ratio $\alpha = M/N$, transmit- and receive-side distortion plus noise covariance matrices $\mathbf{R}_v = r_v \mathbf{I}_M$ and \mathbf{R}_w , respectively, and the average transmit power per antenna $\bar{\gamma}$. Let also the optimization parameter $\tilde{s} > 0$ be given.
- 2) Plug the values of $\{\alpha, \bar{\gamma}, \tilde{s}\}$ to (28) and obtain ξ .
- 3) Insert ξ along with the rest of the necessary parameters in (29) and (30), and solve η numerically, e.g., using iterative substitution method.
- 4) Use the solutions of ξ and η in (31) to obtain the free energy.
- 5) Optimize (27) over $\tilde{s} > 0$.

the transmit-side are spatially uncorrelated, namely, $\Gamma = \bar{\gamma} \mathbf{I}_M$ and $\mathbf{R}_v = r_v \mathbf{I}_M$. The receiver postulates spatially white noise $\tilde{\mathbf{R}} = \tilde{r} \mathbf{I}_N$ with some variance $\tilde{r} > 0$. This allows us to write

$$\frac{1}{M} I_{\text{GMI}}(\mathbf{y}; \mathbf{x}) = \sup_{\tilde{s} > 0} \left\{ f(\tilde{s}) - \alpha^{-1} \tilde{s} [N^{-1} \text{tr}(\mathbf{R}_w) + r_v] \right\}, \quad (27)$$

where $f(\tilde{s})$ is given by (13) with $s\tilde{\mathbf{R}}^{-1}$ replaced by $\tilde{s}\mathbf{I}_N$. Furthermore, in this case all variables are identically distributed for all $m = 1, 2, \dots, M$ so we may omit the subscripts related to m in the following. We still need to fix the input distribution (2) to obtain the parameters (23) and (24). For this, we give two concrete examples: 1) Gaussian signaling; and 2) discrete channel inputs, such as, QAM.

Example 2. Let the channel inputs (2) be IID Gaussian, namely, $p(\mathbf{x}) = g(\mathbf{x} | \mathbf{0}; \bar{\gamma} \mathbf{I}_M)$ so that $p(\tilde{\chi}_m) = p(x_m) = g(x | 0; \bar{\gamma})$ and $p(\chi_m) = g(\chi_m | 0; \bar{\gamma} + r_v)$ in Proposition 1. The parameter ξ can then be obtained explicitly as

$$\xi = \frac{\bar{\gamma} \tilde{s} (1 - \alpha) - \alpha + \sqrt{4\alpha \bar{\gamma} \tilde{s} + [\bar{\gamma} \tilde{s} (1 - \alpha) - \alpha]^2}}{2\alpha \bar{\gamma}}, \quad (28)$$

while η and ε are obtained by solving the coupled fixed point equations

$$\eta = \frac{1}{\alpha [N^{-1} \text{tr}(\mathbf{R}_w) + \varepsilon]}, \quad (29)$$

$$\varepsilon = \frac{\eta r_v + \bar{\gamma}(\eta + \xi^2 \bar{\gamma})}{\eta(1 + \xi \bar{\gamma})^2} = \frac{\bar{\gamma} + r_v}{(1 + \xi \bar{\gamma})^2} + \frac{1}{\eta(1 + 1/\xi \bar{\gamma})^2}. \quad (30)$$

Additional algebra shows that for IID Gaussian inputs, the free energy (26) reduces to

$$f_{\text{RS}}(\tilde{s}) = \frac{1}{\alpha} \left(\frac{\xi}{\eta} + \ln \tilde{s} + \ln \frac{1}{\alpha \xi} \right) - \xi \varepsilon + \ln(1 + \xi \bar{\gamma}) + \frac{\xi r_v}{1 + \xi \bar{\gamma}}. \quad (31)$$

Note that the expression for parameter $\tilde{\varepsilon}$ in (24) is not explicitly given here but it is implicitly a part of (28) due to relations (20) and (22). ◊

The computational formula for obtaining the GMI with the above example is detailed in Table I. Notice that there are two non-trivial steps in the algorithm: 1) the optimization over $s > 0$; and 2) the problem of solving a system of two nonlinear equations with two unknowns. The first difficulty is not specific to the current study and is present in any work that considers GMI as means to analyze mismatched decoding. The computational complexity of the second problem is negligible

compared to the original task of taking an expectation over the channel matrices in (11). Indeed, a typical solution for η and ε is obtained after some tens of iterations of an iterative substitution method. For the high-SNR case where $\bar{\gamma} \rightarrow \infty$ for a fixed covariance matrix \mathbf{R}_w , the result can be further simplified as shown in Example 3 below.

Example 3. Let us consider the case of Gaussian signaling as given in Example 2 in the limit $\bar{\gamma} \rightarrow \infty$. We assume for simplicity (see, e.g., [10]) that $\mathbf{R}_w = r_w \mathbf{I}_N$ and $r_v = \bar{\gamma} \kappa^2$ where $\kappa > 0$ and $r_w > 0$ are fixed and finite parameters. At high-SNR, there are two possibilities for the parameter $\tilde{s} = s/\bar{\gamma}$ in the GMI: 1) the optimal value of \tilde{s} is a strictly positive constant; and 2) the value of \tilde{s} goes to zero when $\bar{\gamma} \rightarrow \infty$. For the first case, $M^{-1} I_{\text{GMI}}^{(s)}(\mathbf{y}; \mathbf{x}) \rightarrow -\infty$ so in order to obtain a consistent solution for the fixed point equations, the parameter \tilde{s} has to be inversely proportional to $\bar{\gamma}$, i.e., $\tilde{s} = s_{\bar{\gamma}}/\bar{\gamma}$ where $s_{\bar{\gamma}}$ is a strictly positive finite constant. Then $\xi \rightarrow 0$ as $\bar{\gamma} \rightarrow \infty$, and the normalized GMI reduces to

$$\frac{1}{M} I_{\text{GMI}}^{\infty}(\mathbf{y}; \mathbf{x}) = \sup_{s_{\bar{\gamma}} > 0} \left\{ \frac{1}{\alpha} \ln \left(\frac{s_{\bar{\gamma}}}{\alpha \xi_{\bar{\gamma}}} \right) + \ln(1 + \xi_{\bar{\gamma}}) + \frac{\kappa^2 \xi_{\bar{\gamma}}}{1 + \xi_{\bar{\gamma}}} - \frac{s_{\bar{\gamma}} \kappa^2}{\alpha} \right\}, \quad (32)$$

in the limit $\bar{\gamma} \rightarrow \infty$. The auxiliary parameter $\xi_{\bar{\gamma}} \triangleq \xi \bar{\gamma} > 0$ is given by

$$\xi_{\bar{\gamma}} = \frac{s_{\bar{\gamma}}(1 - \alpha) - \alpha + \sqrt{4\alpha s_{\bar{\gamma}} + [s_{\bar{\gamma}}(1 - \alpha) - \alpha]^2}}{2\alpha}. \quad (33)$$

Compared to the finite-SNR case in Example 2, the GMI is now directly given by (32). \diamond

The next example provides explicit formulas for the GMI given discrete constellations such as QAM.

Example 4. Let \mathcal{A} be a discrete modulation alphabet with fixed and finite cardinality $|\mathcal{A}|$ and consider the GMI (27). Let the channel inputs x_m be drawn independently and uniformly from \mathcal{A} . The parameters of the decoupled channel model in Proposition 1 can be obtained by first solving ξ and $\tilde{\varepsilon}$ from

$$\xi = \frac{\tilde{s}}{\alpha(1 + \tilde{s}\tilde{\varepsilon})}, \quad (34)$$

$$\tilde{\varepsilon} = \bar{\gamma} - \int q(z) |\langle \tilde{x} \rangle_q|^2 dz, \quad (35)$$

using the following definitions for the decoupled estimator and the postulated channel probability

$$\langle \tilde{x} \rangle_q = \frac{1}{q(z)|\mathcal{A}|} \sum_{\tilde{x} \in \mathcal{A}} \tilde{x} g(z | \tilde{x}; \xi^{-1}), \quad (36)$$

$$q(z) = \frac{1}{|\mathcal{A}|} \sum_{x \in \mathcal{A}} g(z | x; \xi^{-1}), \quad (37)$$

respectively. Note that this implies solving two parameters from two nonlinear equations and can be done, for example, by using iterative substitution method. After obtaining the solutions for ξ (and $\tilde{\varepsilon}$), the rest of the parameters can be

obtained by solving the two coupled equations

$$\eta = \frac{1}{\alpha [N^{-1} \text{tr}(\mathbf{R}_w) + \varepsilon]}, \quad (38)$$

$$\varepsilon = \mathbb{E} \{ |v + x - \langle \tilde{x} \rangle_q|^2 \}, \quad (39)$$

for η and ε , where the expectation is w.r.t. the true joint probability of $\{x, v, z\}$. Finally, the free energy reads

$$f_{\text{RS}}(\tilde{s}) = \frac{1}{\alpha} \left(\frac{\xi}{\eta} + \ln \tilde{s} + \ln \frac{1}{\alpha \xi} \right) - \xi \varepsilon + \frac{\xi(\xi - \eta)}{\eta} \tilde{\varepsilon} - \left(\frac{\xi}{\eta} + \ln \frac{\pi}{\xi} + \int p(z) \ln q(z) dz \right), \quad (40)$$

where we denoted

$$p(z) = \frac{1}{|\mathcal{A}|} \sum_{x \in \mathcal{A}} g(z | x; \eta^{-1} + r_v), \quad (41)$$

for the decoupled PDF of the received signal. \diamond

Notice that the form of η in Example 4 is the same as in Example 2, but the parameter ε has now a different structure. Compared to the Gaussian case, the equivalent result for IID discrete channel inputs looks in general more cumbersome. First of all, we need to solve now two sets of equations instead of just one. They both contain terms that involve $|\mathcal{A}|$ summations and there are also two expectations left to evaluate, one in (35) and another in (39). However, both expectations involve only scalar variables. This is in stark contrast to the original problem that involved computing $|\mathcal{A}|^M$ summations for every channel and noise / distortion realization and taking expectation over the channel and noise that are multidimensional integrals. This makes direct Monte Carlo computation of the GMI for discrete signaling in practice infeasible for large constellations and numbers of antennas.

IV. MATCHED JOINT DECODING

A. Definition and the Special Case of Gaussian Signaling

Let us now consider the case of matched decoding where the correct channel transition probability (5) is utilized at the receiver. The first entropy term in (7) reads

$$\mathbb{E} \{ \ln p(\mathbf{y} | \mathbf{x}, \mathbf{H}) \} = -\mathbb{E}_{\mathbf{H}} \{ \ln \det(\mathbf{R}_w + \mathbf{H} \mathbf{R}_v \mathbf{H}^H) \} - c, \quad (42)$$

where $c = N \ln(e\pi)$. It should be remarked that there is still an expectation left w.r.t. the channel realizations \mathbf{H} in (42). This could be evaluated, for example, using Monte Carlo methods or random matrix theory [26], [27]. For the special case of Gaussian inputs, the identities in Appendix A allow us to partially calculate also the latter entropy term in (7), providing the following result that is useful for Monte Carlo simulations.

Example 5. Let $p(\mathbf{x}) = g(\mathbf{x} | \mathbf{0}; \mathbf{\Gamma})$. Then

$$\frac{1}{M} I(\mathbf{y}; \mathbf{x}) = \frac{1}{M} \mathbb{E}_{\mathbf{H}} \{ \ln \det(\mathbf{R}_w + \mathbf{H}(\mathbf{\Gamma} + \mathbf{R}_v) \mathbf{H}^H) \} - \frac{1}{M} \mathbb{E}_{\mathbf{H}} \{ \ln \det(\mathbf{R}_w + \mathbf{H} \mathbf{R}_v \mathbf{H}^H) \}, \quad (43)$$

is the normalized ergodic MI for matched decoding. \diamond

$$I(\mathbf{y}; \mathbf{x}) = M \ln |\mathcal{A}| - N - \frac{1}{|\mathcal{A}|} \sum_{\mathbf{x} \in \mathcal{A}^M} \mathbb{E}_{\mathbf{v}, \mathbf{w}, \mathbf{H}} \left\{ \ln \left(\sum_{\tilde{\mathbf{x}} \in \mathcal{A}^M} e^{-[\mathbf{H}(\mathbf{x} - \tilde{\mathbf{x}} + \mathbf{v}) + \mathbf{w}]^H (\mathbf{R}_w + \mathbf{H} \mathbf{R}_v \mathbf{H})^{-1} [\mathbf{H}(\mathbf{x} - \tilde{\mathbf{x}} + \mathbf{v}) + \mathbf{w}]} \right) \right\} \quad (44)$$

The above expression is relatively easy to compute also by brute-force Monte Carlo methods since there is only an expectation over the fading. Unfortunately, to the best of our knowledge, the latter entropy term in (7) is mathematically intractable for rigorous methods like random matrix theory when $p(\mathbf{x})$ is an arbitrary distribution that satisfies (2). For example, given discrete inputs as in Example 4, calculating $\mathbb{E}\{\ln p(\mathbf{y} | \mathbf{H})\}$ and combining it with (42) reduces the MI to (44) given at the top of this page. This form is computationally very complex and can be evaluated using Monte Carlo methods only for small number of antennas and simple constellations. To obtain a result for general input distribution $p(\mathbf{x})$ that has lower computational complexity, we use the replica method again. A sketch of the derivation can be found in Appendix C. As before, the results that follow have been written in a simplified form where the assumption of LSL is suppressed for notational simplicity. For finite M and N , the results should therefore be considered as approximations.

B. Analytical Results via the Replica Method

Proposition 2. *Let us write for notational convenience*

$$\chi_m = x_m + v_m, \quad (45)$$

where $m = 1, \dots, M$, $x_m \sim p(x_m)$ and $v_m \sim g(v_m | 0; r_v^{(m)})$ are independent for all m . Let

$$p(z_m | \chi_m) = g(z_m | \chi_m; \eta^{-1}), \quad (46)$$

be a conditional PDF of an AWGN channel whose input is (45) and noise variance is η^{-1} . The conditional mean estimator of χ_m received over this channel reads

$$\langle \chi_m \rangle = \frac{\mathbb{E}_{\chi_m} \{\chi_m p(z_m | \chi_m)\}}{\mathbb{E}_{\chi_m} \{p(z_m | \chi_m)\}}, \quad (47)$$

where the parameter η is given, along with another parameter ε , as the solution to the coupled fixed point equations

$$\eta = \frac{1}{\alpha N} \text{tr} [(\mathbf{R}_w + \varepsilon \mathbf{I}_N)^{-1}], \quad (48)$$

$$\varepsilon = \frac{1}{M} \sum_{m=1}^M [\bar{\gamma}_m + r_v^{(m)} - \mathbb{E}\langle \chi_m \rangle^2]. \quad (49)$$

If we also define a second set of parameters η' and ε' that are solutions to the coupled fixed point equations

$$\eta' = \frac{1}{\alpha N} \text{tr} [(\mathbf{R}_w + \varepsilon' \mathbf{I}_N)^{-1}], \quad (50)$$

$$\varepsilon' = \frac{1}{M} \sum_{m=1}^M \frac{r_v^{(m)}}{1 + \eta' r_v^{(m)}}, \quad (51)$$

the per-stream MI is finally given by

$$\frac{1}{M} I(\mathbf{y}; \mathbf{x}) = \frac{\ln \det(\mathbf{R}_w + \varepsilon \mathbf{I}_N) - \ln \det(\mathbf{R}_w + \varepsilon' \mathbf{I}_N)}{\alpha N} - (\eta \varepsilon - \eta' \varepsilon') + \frac{1}{M} \sum_{m=1}^M [I(z_m; \chi_m) - \ln(1 + \eta' r_v^{(m)})], \quad (52)$$

where $I(z_m; \chi_m)$ is the MI of the Gaussian channel defined by (45) and (46).

Proof: An outline of the derivation is given in Appendix C. ■

Just like Proposition 1 in Section III, Proposition 2 is valid for any input distribution that satisfies (2). For concreteness, we again give examples for Gaussian and discrete signaling when the noise plus distortion is spatially white $\mathbf{R}_v = r_v \mathbf{I}_M$ and transmit power is uniformly allocated $\mathbf{\Gamma} = \bar{\gamma} \mathbf{I}_M$. This makes the channels $m = 1, 2, \dots, M$ identically distributed so we omit the subscript m in the following.

Example 6. Let $\mathbf{R}_v = r_v \mathbf{I}_M$ and consider the special case of Gaussian inputs $p(\mathbf{x}) = g(\mathbf{x} | \mathbf{0}; \bar{\gamma} \mathbf{I}_M)$. Then

$$I(z; \chi) = \ln [1 + \eta(\bar{\gamma} + r_v)], \quad (53)$$

$$\varepsilon = \frac{\bar{\gamma} + r_v}{1 + \eta(\bar{\gamma} + r_v)}, \quad (54)$$

and the rest of the parameters are given in Proposition 2. ◇

We next consider the high-SNR case $\bar{\gamma} \rightarrow \infty$ as in Example 3 and compare it to the result obtained in [10] using completely different mathematical methods.

Example 7. For the case $\mathbf{R}_w = r_w \mathbf{I}$, $\mathbf{R}_v = \kappa^2 \bar{\gamma} \mathbf{I}$ (see, e.g., [10]) we find that if $\alpha \leq 1$ then $\bar{\gamma} \rightarrow \infty$ yields $\eta = \eta'$ and $\varepsilon = \varepsilon'$. The high SNR limit is therefore

$$\frac{1}{M} I^\infty(\mathbf{y}; \mathbf{x}) = \log \left(\frac{1 + \kappa^2}{\kappa^2} \right), \quad \alpha \leq 1. \quad (55)$$

For the case $\alpha > 1$, both η and η' tend to zero at high SNR while ε and ε' grow without bound. This is not yet sufficient to solve (52). However, combining this with the relations $\eta' \varepsilon' = \eta \varepsilon$ and $\varepsilon' = \varepsilon \frac{\kappa^2}{1 + \kappa^2}$, that hold in the limit $\bar{\gamma} \rightarrow \infty$ for $\alpha > 1$, provides the second part of the high SNR result

$$\frac{1}{M} I^\infty(\mathbf{y}; \mathbf{x}) = \frac{1}{\alpha} \log \left(\frac{1 + \kappa^2}{\kappa^2} \right), \quad \alpha > 1. \quad (56)$$

The asymptotic mutual information expressions in (55) and (56) coincide exactly with the results obtained previously in [10], as expected. ◇

Example 8. If the channel inputs are from a discrete alphabet \mathcal{A} as in Example 4, the parameter ε in (49) is obtained using

$$\langle \chi \rangle = \frac{1}{p(z)} \sum_{x \in \mathcal{A}} \left[\frac{1}{|\mathcal{A}|} g(z | x; \eta^{-1} + r_v) \left(\frac{x + \eta r_v z}{1 + \eta r_v} \right) \right], \quad (57)$$

$$\mathbb{E}\langle \chi \rangle^2 = \int p(z) \mathbb{E}\{|\langle \chi \rangle|^2\} dz, \quad (58)$$

in Proposition 2. Here $p(z)$ is given by (41) and $\langle \chi \rangle$ denotes the conditional mean estimator of (45) from the observations (46). The related MI term reads by definition

$$I(z; \chi) = \ln \left(\frac{\eta}{e\pi} \right) - \int p(z) \ln p(z) dz. \quad (59)$$

Both (49) and (59) need, in general, to be solved numerically. \diamond

V. NUMERICAL EXAMPLES

In the following, assume for simplicity that $\mathbf{\Gamma} = \bar{\gamma}\mathbf{I}$, $\mathbf{R}_w = \mathbf{I}$ and $\mathbf{R}_v = \kappa^2\bar{\gamma}\mathbf{I}$, where $\kappa = 10^{\text{EVM}_{\text{dB}}/20}$. The SNR without transmit-side noise is therefore simply $\bar{\gamma}$, or in decibels $\bar{\gamma}_{\text{dB}} = 10\log_{10}\bar{\gamma}$. The parameter EVM_{dB} gives the error-vector magnitude of the transmitter in decibels. Furthermore, all cases assume a symmetric antenna setup $\alpha = M/N = 1$ for simplicity because α is not a central parameter for the research problem at hand.

The first numerical experiment plotted in Fig. 2 examines the accuracy of the asymptotic analytical results when applied to finite-sized systems. The EVM is fixed to a rather pessimistic value $\text{EVM}_{\text{dB}} = -10$ to highlight the differences between the ideal and imperfect hardware configurations. The normalized rate is shown using the asymptotic replica analysis (lines) and Monte Carlo simulations (markers) for a finite-size symmetric antenna setup with $M = N = 4$. In the case of Gaussian signaling, plotted in Fig. 2(a), the analytical approximations for the normalized rate $M^{-1}I(\mathbf{y}; \mathbf{x})$ given by Examples 2 and 6 are quite good when compared to the finite size simulations based on Examples 1 and 5. For discrete signaling depicted in Fig. 2(b) we have plotted only the case of matched decoding due to the computational complexity of Monte Carlo simulations in the mismatched case. The gap between asymptotic result presented in Example 8 and Monte Carlo averaging of (44) is similar to the Gaussian case for both constellations. Figure 2 shows that the analytical approximation given by the replica method is reasonably good already at $M = N = 4$, even though formally the limit $M, N \rightarrow \infty$ is required by the analysis.

The next example in Fig. 3 illustrates the performance of an $M = N$ MIMO system for a more realistic EVM value $\text{EVM}_{\text{dB}} = -20$. For the case of matched decoding we used Examples 6 and 8, while Examples 2 and 4 were used to obtain the curves representing mismatched decoding. In Fig. 3(a), the normalized rate $M^{-1}I(\mathbf{y}; \mathbf{x})$ is depicted as a function of SNR $\bar{\gamma}_{\text{dB}}$. For clarity of presentation, we have plotted only the ideal case and the case of non-ideal hardware with matched decoding. Note that the Gaussian curves (black lines) here are the same as the simulation curves in [10, Fig. 2] given the parameter value $\kappa = 0.1$. Apart from 64-QAM and Gaussian signaling, the figure seems to imply that lower order constellations exhaust the source entropy before the transmit-side noise has any significant effect for this choice of EVM. To see more clearly the effect of transmit noise, Fig. 3(b) shows the rate loss (in percents) for the case with transmit noise $\text{EVM}_{\text{dB}} = -20$ when compared to the ideal case $\text{EVM}_{\text{dB}} = -\infty$. The solid lines represent again matched decoding while dash-dotted lines are for mismatched decoding. As expected, mismatch decoding reduces the achievable

rate when compared to matched decoding, but the effect is relatively minor when compared to the total rate loss caused by the presence of transmit noise itself. The markers depict the points where maximum relative rate loss is experienced for matched decoding. Same markers are also plotted in Fig. 3(a) for comparison.

In Fig. 4 we have plotted the asymptotic high-SNR results given in Examples 3 and 7. Note that given a finite value of EVM_{dB} , the normalized rates for matched and mismatched decoding have a gap in this case. For more realistic, but still quite high SNR values of 20 dB and 30 dB, the two decoding strategies converge to the same value roughly when $\bar{\gamma}_{\text{dB}} < -\text{EVM}_{\text{dB}}$. The apparent discrepancy is explained by recalling that the asymptotic cases assume $\bar{\gamma} \rightarrow \infty$ for a fixed and nonzero EVM and, thus, as a finite SNR approximation implies $\bar{\gamma} \gg 1/\kappa^2$. As may be observed from the lower right corner of the figure, the SNR values 20 dB and 30 dB have also a similar behavior near $\bar{\gamma} \gg 1/\kappa^2$. Thus, the high-SNR result is consistent with the finite-SNR cases.

It is important to guarantee certain performance when designing a system. The maximum EVM that leads to at most 5 % rate loss (as compared to having ideal hardware) for a fixed input distribution and different given SNRs is plotted in Fig. 5. For Gaussian signaling we have plotted both the matched and mismatched cases while discrete cases assume matched joint decoding for simplicity. As expected, the EVM requirement for Gaussian signaling is a monotonically decreasing, but not linear, function of SNR. A simple linear approximation that provides a lower bound for the case of Gaussian signaling with matched decoding is given by $\text{EVM}_{\text{dB}} = -0.7 \cdot \bar{\gamma}_{\text{dB}} - 13$ for the depicted region. This can be used as a simple rule-of-thumb for worst case maximum allowed EVM in the system. For discrete constellations, the EVM requirement first follows the Gaussian case but then starts to get looser at higher SNRs. This is expected, as can be observed from Fig. 3(a), since the maximum achievable rate for a discrete constellation saturates at a certain SNR when the input distribution runs out of entropy. After this point, the rate loss can be held fixed for increasing SNR by increasing the transmit-side noise variance, or EVM, accordingly.

VI. CONCLUSIONS

Considering a ‘binoisy’ channel model, we have derived asymptotic expressions for the achievable rate of MIMO systems suffering from transceiver hardware impairments. For matched decoding, where the receiver is designed and implemented explicitly based on the generalized system model, expressions for the ergodic mutual information between the channel inputs and outputs have been given. In addition, a simplified receiver that neglected the hardware imperfections and performed mismatched detection and decoding has been studied via generalized mutual information. The mathematical expressions provided in the paper cover practical discrete modulation schemes, such as, quadrature amplitude modulation, as well as Gaussian signaling. The numerical results showed that for realistic system parameters, the effects of transmit-side noise and mismatched decoding become significant only at

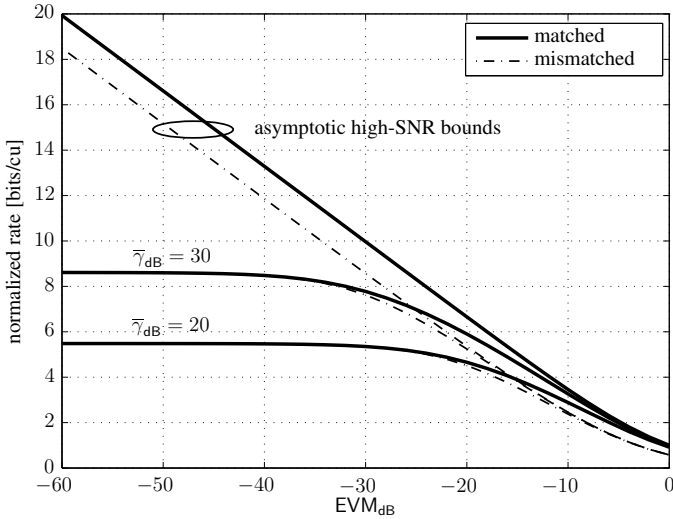


Fig. 4. Normalized rate $M^{-1}I(\mathbf{y}; \mathbf{x})$ in bits per channel use vs. EVM in decibels for MIMO transmission with Gaussian signaling. Solid lines for matched decoding and dash-dotted lines for mismatched decoding.

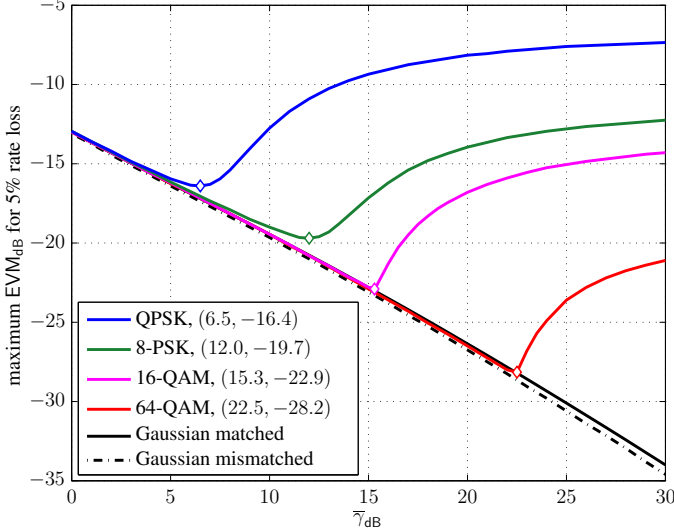


Fig. 5. Maximum allowed EVM in decibels for matched decoding so that the system experiences at most 5% loss in rate compared to the case with ideal hardware ($\text{EVM}_{\text{dB}} = -\infty$). Markers depict the worst case EVM requirement for the discrete constellations and parenthesis in the legend provide the respective values as $(\bar{\gamma}_{\text{dB}}, \text{EVM}_{\text{dB}})$. All discrete cases correspond to matched joint decoding at the receiver.

high modulation orders. Furthermore, the effect of mismatched decoding was found to be relatively minor compared to the total rate loss caused by the presence of transmit noise itself. The results were also used to identify the maximum EVM values that allows for certain system operation.

APPENDIX A USEFUL RESULTS

The Gaussian integration formula for $\mathbf{x} \in \mathbb{C}^N$ reads

$$\frac{1}{\pi^N} \int e^{-\mathbf{x}^H \mathbf{M} \mathbf{x} + 2\Re\{\mathbf{b}^H \mathbf{x}\}} d\mathbf{x} = \frac{1}{\det(\mathbf{M})} e^{\mathbf{b}^H \mathbf{M}^{-1} \mathbf{b}}. \quad (60)$$

For suitable matrices, the identity

$$\begin{aligned} & (\mathbf{W}^{-1} + \mathbf{U}\mathbf{T}^{-1}\mathbf{V}^H)^{-1} \\ &= \mathbf{W} - \mathbf{W}\mathbf{U}(\mathbf{T} + \mathbf{V}^H\mathbf{W}\mathbf{U})^{-1}\mathbf{V}^H\mathbf{W}, \end{aligned} \quad (61)$$

and the related determinant identity

$$\begin{aligned} \det(\mathbf{W}^{-1} + \mathbf{U}\mathbf{T}^{-1}\mathbf{V}^H) \\ = \det(\mathbf{T} + \mathbf{V}^H\mathbf{W}\mathbf{U}) \det(\mathbf{W}^{-1}) \det(\mathbf{T}^{-1}), \end{aligned} \quad (62)$$

are also useful, along with

$$\frac{\partial}{\partial x} \ln \det \mathbf{A} = \text{tr} \left(\mathbf{A}^{-1} \frac{\partial \mathbf{A}}{\partial x} \right), \quad (63)$$

$$\text{tr} [\mathbf{A}^{-1} - (\mathbf{A} + \mathbf{B})^{-1}] = \text{tr} [\mathbf{A}^{-1} \mathbf{B} (\mathbf{A} + \mathbf{B})^{-1}], \quad (64)$$

where the partial derivative in (63) should be understood as an elementwise operation on \mathbf{A} .

APPENDIX B REPLICA ANALYSIS FOR MISMATCHED CASE

Let us consider the function $f(s)$ (free-energy) defined in (13). We then postulate that it can be expressed using the standard replica trick [21], [22] as

$$f(s) = - \lim_{M \rightarrow \infty} \frac{1}{M} \lim_{u \rightarrow 0} \frac{\partial}{\partial u} \ln \Xi^{(u, M)}(s), \quad (65)$$

where we defined for later convenience

$$\Xi^{(u, M)}(s) = \mathbb{E} \exp \left[- \sum_{a=1}^u (\mathbf{w} + \Delta_a)^H \Sigma^{-1} (\mathbf{w} + \Delta_a) \right]. \quad (66)$$

We also denoted $\Sigma = s^{-1} \tilde{\mathbf{R}}$ and $\Delta_a = \mathbf{H}(\mathbf{x}_0 + \mathbf{v}_0) - \mathbf{H}\mathbf{x}_a = \mathbf{H}\chi_0 - \mathbf{H}\chi_a$, where χ_0, χ_a have the obvious definitions. Here \mathbf{x}_0 is the original transmit vector in (1) and $\{\mathbf{x}_a\}_{a=1}^u$ are replicated data vectors, which are IID drawn according to $p(\mathbf{x})$ when conditioned on $\{\mathbf{x}_0, \mathbf{v}_0, \mathbf{w}, \mathbf{H}\}$. On the other hand, \mathbf{v}_0 represents the noise plus distortion component at the transmit-side that is CSCG with covariance matrix \mathbf{R}_v . It can be readily noticed that the above formulation is mathematically somewhat problematic since (65) assumes $u \in \mathbb{R}$ while in (66) it is an integer. Thus, the replica trick assumes the existence of some form of analytical continuation although the proof of its existence is in general an open problem (see, e.g., [20]–[22]). Starting with (66), the goal is then to obtain a functional expression for $\Xi^{(u, M)}(s)$ in the LSL that does not enforce u to be an integer and then use (65) to obtain the desired quantity. In the following, explicit limit notations are often omitted for notational convenience.

To proceed with the evaluation of (66), we first make the RS assumption

$$p = M^{-1} \|\chi_0\|^2, \quad (67)$$

$$m = M^{-1} \chi_0^H \chi_a, \quad a = 1, \dots, u, \quad (68)$$

$$Q = M^{-1} \|\chi_a\|^2, \quad a = 1, \dots, u, \quad (69)$$

$$q = M^{-1} \chi_a^H \chi_b, \quad a \neq b \in \{1, \dots, u\}, \quad (70)$$

and remark that

$$\mathbb{E}_H \{\Delta_a \Delta_b^H\} = \begin{cases} [p - (m + m^*) + Q] \mathbf{I}_N, & a = b, \\ [p - (m + m^*) + q] \mathbf{I}_N, & a \neq b, \end{cases} \quad (71)$$

since the channel matrices are assumed to have IID elements. Note that the empirical correlations between $\{\mathbf{x}_a\}_{a=0}^u$ are not

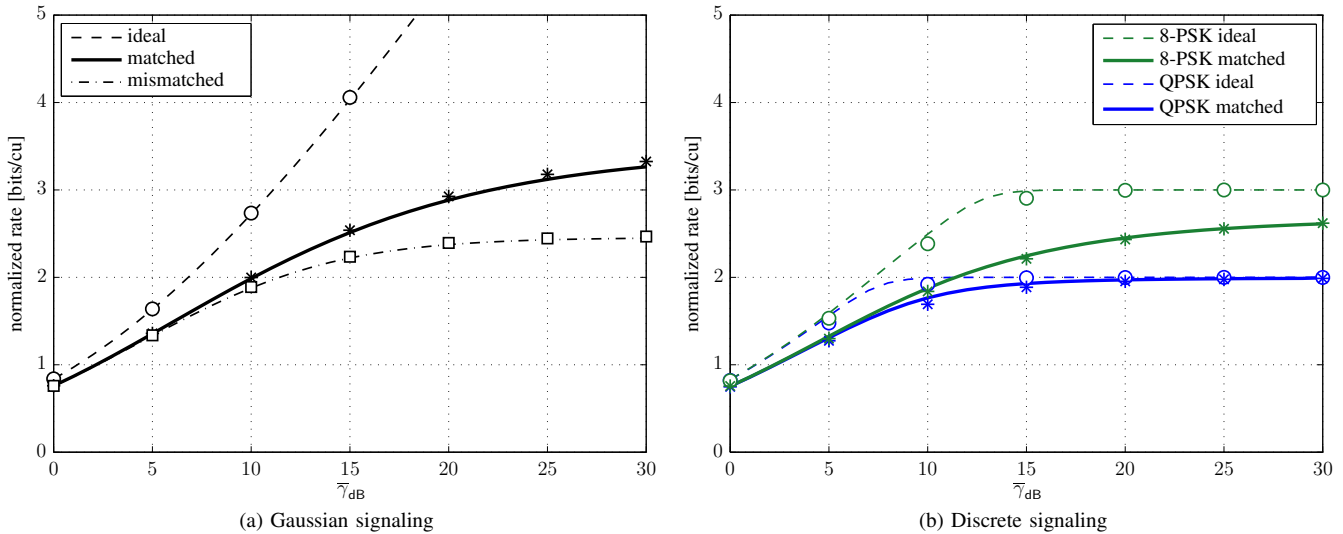


Fig. 2. Normalized rate $M^{-1}I(\mathbf{y}; \mathbf{x})$ in bits per channel use (cu) vs. SNR for MIMO transmission. Lines for replica results and markers for Monte Carlo simulations for $M = N = 4$ antenna configuration. Selected cases of ideal hardware $\text{EVM}_{\text{dB}} = -\infty$ and hardware impairments ($\text{EVM}_{\text{dB}} = -10$) with matched and mismatched decoding are plotted.

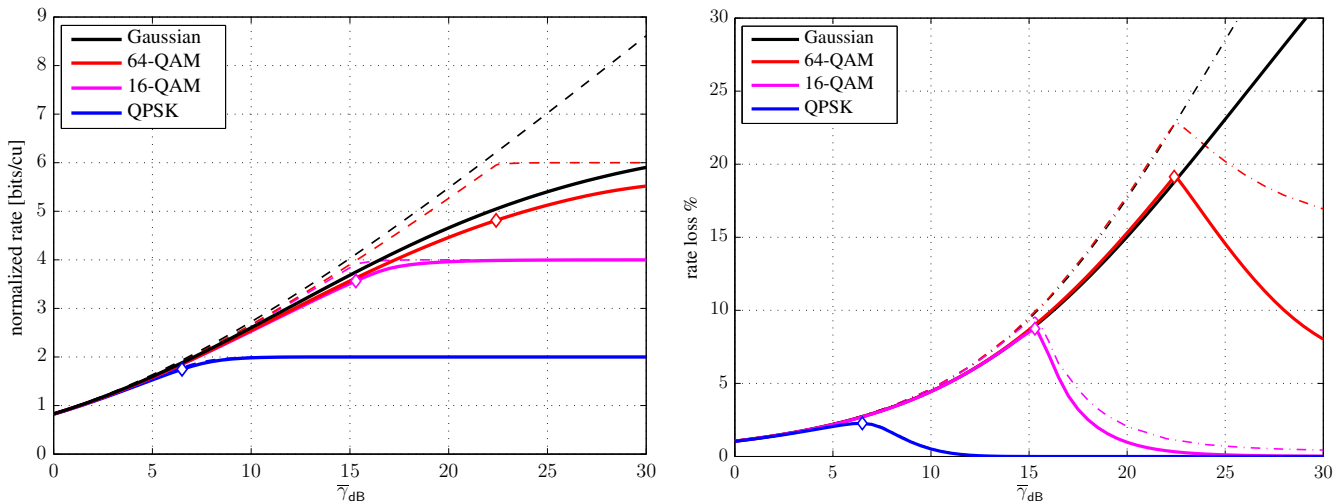


Fig. 3. Performance of a MIMO system with $M = N$ antennas and given ideal ($\text{EVM}_{\text{dB}} = -\infty$) or non-ideal hardware ($\text{EVM}_{\text{dB}} = -20$) for different signaling methods. Markers depict the points where discrete constellations and matched decoding with hardware impairments experience the maximum rate losses compared to the ideal cases.

in general zero due to the expectation w.r.t. \mathbf{H} . As $M = \alpha N \rightarrow \infty$, we may replace $\{\Delta_a\}_{a=1}^u$ by

$$\Delta_a = \mathbf{d}_a \sqrt{Q} - q + \mathbf{t} \sqrt{p - (m + m^*) + q} \quad (72)$$

$$= \mathbf{d}_a \sqrt{A} + \mathbf{t} \sqrt{B}, \quad (73)$$

where $\{\mathbf{t}, \{\mathbf{d}_a\}_{a=1}^u\}$ are IID standard complex Gaussian RVs independent of \mathbf{w} . Plugging (73) into $\Xi^{(u,M)}(s)$ gives

$$\begin{aligned} \Xi^{(u,M)}(s) &= \frac{1}{\det(\mathbf{R}_w)} \mathbb{E} \int \frac{d\mathbf{w}}{\pi^N} e^{-\mathbf{w}^H (\mathbf{R}_w^{-1} + u\mathbf{\Sigma}^{-1}) \mathbf{w}} \\ &\times \int \frac{d\mathbf{t}}{\pi^N} e^{-\mathbf{t}^H (\mathbf{I} + uB\mathbf{\Sigma}^{-1}) \mathbf{t} - 2\Re\{\mathbf{w}^H (u\sqrt{B}\mathbf{\Sigma}^{-1}) \mathbf{t}\}} \\ &\times \left[\int e^{-\mathbf{d}^H (\mathbf{I} + A\mathbf{\Sigma}^{-1}) \mathbf{d} + 2\Re\{[-\sqrt{A}\mathbf{\Sigma}^{-1}(\mathbf{w} + \sqrt{B}\mathbf{t})]^H \mathbf{d}\}} \frac{d\mathbf{d}}{\pi^N} \right]^u. \end{aligned} \quad (74)$$

Next, the Gaussian integration formula (60) is applied on the integral w.r.t. \mathbf{d} . With the help of (61) we arrive at

$$\begin{aligned} \Xi^{(u,M)}(s) &= \mathbb{E} \int \frac{d\mathbf{w}}{\pi^N} \frac{e^{-\mathbf{w}^H (\mathbf{R}_w^{-1} + u(\mathbf{A}\mathbf{I}_N + \mathbf{\Sigma})^{-1}) \mathbf{w}}}{[\det(\mathbf{I} + A\mathbf{\Sigma}^{-1})]^u \det(\mathbf{R}_w)} \\ &\times \int e^{-\mathbf{t}^H [\mathbf{I}_N + uB(\mathbf{A}\mathbf{I}_N + \mathbf{\Sigma})^{-1}] \mathbf{t} + 2\Re\{[-u\sqrt{B}(\mathbf{A}\mathbf{I}_N + \mathbf{\Sigma})^{-1} \mathbf{w}]^H \mathbf{t}\}} \frac{d\mathbf{t}}{\pi^N}. \end{aligned} \quad (75)$$

Using (60) and (61) again for the integral w.r.t. t provides

$$\begin{aligned} & \Xi^{(u,M)}(s) \\ &= \mathbb{E} \left\{ \frac{[\det(\mathbf{I} + A\boldsymbol{\Sigma}^{-1})]^{-u}}{\det[\mathbf{I}_N + uB(A\mathbf{I}_N + \boldsymbol{\Sigma})^{-1}] \det(\mathbf{R}_w)} \right. \\ & \quad \left. \times \int e^{-\mathbf{w}^H (\mathbf{R}_w^{-1} + u[(A+uB)\mathbf{I}_N + \boldsymbol{\Sigma}]^{-1}) \mathbf{w}} \frac{d\mathbf{w}}{\pi^N} \right\} \\ &= \mathbb{E} \left\{ \frac{(\det[\mathbf{I}_N + u\mathbf{R}_w((A+uB)\mathbf{I}_N + \boldsymbol{\Sigma})^{-1}])^{-1}}{\det[\mathbf{I}_N + uB(A\mathbf{I}_N + \boldsymbol{\Sigma})^{-1}] [\det(\mathbf{I} + A\boldsymbol{\Sigma}^{-1})]^u} \right\}, \end{aligned} \quad (76)$$

where the second line comes again from the Gaussian integration formula. Note that this holds for any \mathbf{R}_w and $\boldsymbol{\Sigma}$ that are Hermitian and invertible. The determinants in (76) can be further simplified using (62). Recalling $\boldsymbol{\Sigma} = s^{-1}\tilde{\mathbf{R}}$ and defining two auxiliary matrices

$$\boldsymbol{\Omega}(p, m, q) = \mathbf{R}_w + (p - (m + m^*) + q)\mathbf{I}_N, \quad (77)$$

$$\tilde{\boldsymbol{\Omega}}(Q, q) = s^{-1}\tilde{\mathbf{R}} + (Q - q)\mathbf{I}_N, \quad (78)$$

that are both Hermitian, we finally have

$$\Xi^{(u,M)}(s) = \det(s^{-1}\tilde{\mathbf{R}})^u \mathbb{E} \{ e^{G^{(u)}(p, m, q, Q)} \}, \quad (79)$$

where the auxiliary function

$$\begin{aligned} G^{(u)}(p, m, q, Q) &= (1 - u) \ln \det \tilde{\boldsymbol{\Omega}}(Q, q) \\ & \quad - \ln \det [\tilde{\boldsymbol{\Omega}}(Q, q) + u\boldsymbol{\Omega}(p, m, q)], \end{aligned} \quad (80)$$

turns out to be useful in the sequel. Using the results in Appendix A, we also obtain for later use the equalities

$$\frac{\partial}{\partial p} G^{(u)}(\mathbf{Q}) = -u \operatorname{tr} ((\tilde{\boldsymbol{\Omega}} + u\boldsymbol{\Omega})^{-1}), \quad (81)$$

$$\frac{\partial}{\partial m} G^{(u)}(\mathbf{Q}) = \frac{\partial}{\partial m^*} G^{(u)}(\mathbf{Q}) = u \operatorname{tr} ((\tilde{\boldsymbol{\Omega}} + u\boldsymbol{\Omega})^{-1}), \quad (82)$$

$$\frac{\partial}{\partial q} G^{(u)}(\mathbf{Q}) = u(u-1) \operatorname{tr} (\tilde{\boldsymbol{\Omega}}^{-1} \boldsymbol{\Omega} (\tilde{\boldsymbol{\Omega}} + u\boldsymbol{\Omega})^{-1}), \quad (83)$$

$$\frac{\partial}{\partial Q} G^{(u)}(\mathbf{Q}) = u \operatorname{tr} (\tilde{\boldsymbol{\Omega}}^{-1} \boldsymbol{\Omega} (\tilde{\boldsymbol{\Omega}} + u\boldsymbol{\Omega})^{-1}) - u \operatorname{tr} (\tilde{\boldsymbol{\Omega}}^{-1}), \quad (84)$$

where we wrote for notational simplicity $\boldsymbol{\Omega} = \boldsymbol{\Omega}(p, m, q)$, $\tilde{\boldsymbol{\Omega}} = \tilde{\boldsymbol{\Omega}}(Q, q)$ and $G^{(u)}(\mathbf{Q}) = G^{(u)}(p, m, q, Q)$.

Let us now return to (71) and write the general form of empirical correlations between the replicated vectors as

$$\begin{aligned} \frac{1}{M} \mathbb{E}_H \{ \boldsymbol{\Delta}_b^H \boldsymbol{\Delta}_a \} &= \left(\frac{\|\boldsymbol{\chi}_0\|^2}{M} - \frac{\boldsymbol{\chi}_b^H \boldsymbol{\chi}_0}{M} - \frac{\boldsymbol{\chi}_0^H \boldsymbol{\chi}_a}{M} + \frac{\boldsymbol{\chi}_b^H \boldsymbol{\chi}_a}{M} \right) \\ &= (Q_{0,0} - Q_{0,b} - Q_{a,0} + Q_{a,b}), \end{aligned} \quad (85)$$

where the variables $Q_{a,b}$ have the obvious definitions. For future convenience, denote $\mathbf{Q} \in \mathbb{C}^{(u+1) \times (u+1)}$ for the matrix whose (a, b) th component is $Q_{a,b}$. The road map ahead is to first use (85) in determining the probability weight of the matrix \mathbf{Q} and at a suitable point recall the RS assumption (67)–(70) to finish the derivation.

By definition,

$$\mu(\mathbf{Q}) = \mathbb{E} \left\{ \prod_{a=0}^u \prod_{b=a+1}^u \delta(MQ_{a,b} - \boldsymbol{\chi}_b^H \boldsymbol{\chi}_a) \right\}. \quad (86)$$

If $M, N \rightarrow \infty$ with fixed ratio $\alpha = M/N$, we may evaluate (86) using the large deviations theory. By Assumption 1, the elements of $\boldsymbol{\chi}_a$ are independent zero-mean and of bounded variance for all $a = 0, 1, \dots, u$. Thus, the Gärtner-Ellis Theorem [28] states that $\mu(\mathbf{Q})$ satisfies the large deviation property with rate function

$$c^{(u)}(\mathbf{Q}) = \operatorname{extr}_{\tilde{\mathbf{Q}}} \left\{ \operatorname{tr}(\mathbf{Q}\tilde{\mathbf{Q}}) - \lim_{M \rightarrow \infty} \frac{1}{M} \sum_{m=1}^M \ln \phi_m^{(u)}(\tilde{\mathbf{Q}}) \right\}, \quad (87)$$

where $\tilde{\mathbf{Q}}$ has the same form as \mathbf{Q} ,

$$\phi_m^{(u)}(\tilde{\mathbf{Q}}) = \mathbb{E}_{\{\chi_{a,m}\}} \left\{ \exp \left[\sum_{a=0}^u \sum_{b=0}^u \tilde{Q}_{a,b} \chi_{a,m}^* \chi_{a,m} \right] \right\}, \quad (88)$$

and $\boldsymbol{\chi}_a = [\chi_{a,1} \cdots \chi_{a,M}]^\top$.

By the RS assumption, the trace in (87) simplifies as

$$\operatorname{tr}(\mathbf{Q}\tilde{\mathbf{Q}}) = p\tilde{p} + u(m\tilde{m}^* + \tilde{m}m^*) + uQ\tilde{Q} + u(u-1)q\tilde{q}, \quad (89)$$

and we may write the free energy using Varadhan's Lemma [28] as in (90) at the top of the next page. The first set of saddle points arise from

$$\frac{\partial}{\partial x} \operatorname{tr}(\mathbf{Q}\tilde{\mathbf{Q}}) = \frac{1}{M} \frac{\partial}{\partial x} G^{(u)}(\mathbf{Q}), \quad (91)$$

for $x \in \{p, m^*, q, Q\}$. The partial derivatives on the LHS are trivial due to (89) and the RHSs we already obtained in (81)–(84). If we drop the explicit dependence of $\boldsymbol{\Omega}$ and $\tilde{\boldsymbol{\Omega}}$ on $\{p, m, q, Q\}$ for notational simplicity, the RS conjugate parameters at the saddle point thus satisfy

$$\tilde{p} = -u \frac{1}{M} \operatorname{tr} [(\tilde{\boldsymbol{\Omega}} + u\boldsymbol{\Omega})^{-1}] = -u\tilde{m}, \quad (92)$$

$$\tilde{m} = \frac{1}{M} \operatorname{tr} [(\tilde{\boldsymbol{\Omega}} + u\boldsymbol{\Omega})^{-1}], \quad (93)$$

$$\tilde{q} = \frac{1}{M} \operatorname{tr} [\tilde{\boldsymbol{\Omega}}^{-1} \boldsymbol{\Omega} (\tilde{\boldsymbol{\Omega}} + u\boldsymbol{\Omega})^{-1}], \quad (94)$$

$$\tilde{Q} = \frac{1}{M} \operatorname{tr} [\tilde{\boldsymbol{\Omega}}^{-1} \boldsymbol{\Omega} (\tilde{\boldsymbol{\Omega}} + u\boldsymbol{\Omega})^{-1}] - \frac{1}{M} \operatorname{tr} (\tilde{\boldsymbol{\Omega}}^{-1}). \quad (95)$$

Note that the above implies $\tilde{m} = \tilde{m}^* \in \mathbb{R}$ and in the limit $u \rightarrow 0$, we have $\tilde{p} \rightarrow 0$, and $\tilde{m} \rightarrow -(\tilde{Q} - \tilde{q})$. For future convenience, we also remark that

$$\lim_{u \rightarrow 0} \frac{\partial}{\partial u} \tilde{p} = -\frac{1}{M} \operatorname{tr} (\tilde{\boldsymbol{\Omega}}^{-1}) = -\tilde{m}|_{u \rightarrow 0}. \quad (96)$$

The next task is to obtain an explicit expression for the per-component moment generating function (MGF) in (88) that does not require u to be an integer. Since this part is closely similar to the analysis carried out, e.g., in [22] we omit the details of the derivations. Following the notation of [22], we let $\xi = \tilde{m}$ and $\eta = \tilde{m}^2/\tilde{q}$. Then, recalling $\chi_m = x_m + v_m$ and $\tilde{\chi}_m = \tilde{x}_m$

$$\begin{aligned} \phi_m^{(u)}(\tilde{\mathbf{Q}}) &= \left(\frac{\pi}{\xi} \right)^u \mathbb{E} \left\{ \int dz_m e^{u\xi(|z_m|^2 - |\chi_m|^2)} \right. \\ & \quad \left. \times p(z_m | \chi_m) [E_{\tilde{\chi}_m} q(z_m | \tilde{\chi}_m)]^u \right\}, \end{aligned} \quad (97)$$

where $p(z_m | \chi_m) = g(z_m | \chi_m; \eta^{-1})$ and $q(z_m | \tilde{\chi}_m) = g(z_m | \tilde{\chi}_m; \xi^{-1})$. As a consequence of the above, u does not need to be an integer anymore and the limit $u \rightarrow 0$ is well

$$f_{\text{RS}} = - \lim_{M \rightarrow \infty} \frac{1}{M} \ln \det(\mathbf{\Sigma}) - \text{extr}_{\mathbf{Q}, \tilde{\mathbf{Q}}} \lim_{M \rightarrow \infty} \left\{ \frac{1}{M} \lim_{u \rightarrow 0} \frac{\partial}{\partial u} G^{(u)}(\mathbf{Q}) \right. \\ \left. - \lim_{u \rightarrow 0} \frac{\partial}{\partial u} [p\tilde{p} + u(m\tilde{m}^* + \tilde{m}m^*) + uQ\tilde{Q} + u(u-1)q\tilde{q}] + \frac{1}{M} \sum_{m=1}^M \lim_{u \rightarrow 0} \frac{\partial}{\partial u} \ln \phi_m^{(u)}(\tilde{\mathbf{Q}}) \right\} \quad (90)$$

defined. From the partial derivatives of $\{\tilde{p}, \tilde{m}, \tilde{q}, \tilde{\mathbf{Q}}\}$ we obtain the second set of saddle-point conditions

$$p = \lim_{M \rightarrow \infty} \frac{1}{M} \sum_{m=1}^M \mathbb{E}|x_m + v_m|^2, \quad (98)$$

$$Q = \lim_{M \rightarrow \infty} \frac{1}{M} \sum_{m=1}^M \mathbb{E}\langle |\tilde{x}_m|^2 \rangle_q, \quad (99)$$

$$m = \lim_{M \rightarrow \infty} \frac{1}{M} \sum_{m=1}^M \mathbb{E}(x_m + v_m) \langle \tilde{x}_m^* \rangle_q, \quad (100)$$

$$q = \lim_{M \rightarrow \infty} \frac{1}{M} \sum_{m=1}^M \mathbb{E}\langle \tilde{x}_m^* \rangle_q \langle \tilde{x}_m^* \rangle_q, \quad (101)$$

where $x_m, \tilde{x}_m \sim p(x_m)$, $v_m \sim g(v_m | 0; r_v^m)$,

$$\langle f(\tilde{x}_m) \rangle_q = \mathbb{E}_{\tilde{x}_m} f(\tilde{x}_m) \frac{q(z_m | \tilde{x}_m)}{q(z_m)}, \quad (102)$$

and $q(z_m) = \mathbb{E}_{\tilde{x}_m} q(z_m | \tilde{x}_m)$. Clearly the order parameters $\{p, m, q, Q\}$ do not anymore depend on u being integer valued, as desired. This may be interpreted so that (102) is the conditional mean estimator for the postulated Gaussian channel $q(z_m | \tilde{x}_m)$, while the received symbol is obtained through the true channel $p(z_m | \chi_m)$. Then

$$\varepsilon = p - (m + m^*) + q, \quad (103)$$

$$\tilde{\varepsilon} = Q - q, \quad (104)$$

are the true and postulated MMSE of the data given a mismatched decoder as given in (23) and (24), respectively.

The previous analysis obtained the macroscopic parameters that define the RS free energy in the LSL in the limit $u \rightarrow 0$. To obtain the free energy itself, we need to solve the final partial derivatives in (90). Using (63) we have

$$\frac{1}{M} \lim_{u \rightarrow 0} \frac{\partial}{\partial u} G^{(u)}(\mathbf{Q}) = -\frac{1}{M} \ln \det \tilde{\mathbf{\Omega}} - \frac{1}{M} \text{tr}(\tilde{\mathbf{\Omega}}^{-1} \mathbf{\Omega}), \quad (105)$$

and with some algebra one also obtains

$$\frac{\partial}{\partial u} [p\tilde{p} + u(m\tilde{m}^* + \tilde{m}m^*) + uQ\tilde{Q} + u(u-1)q\tilde{q}] \Big|_{u \rightarrow 0} \\ = -\xi\varepsilon + \frac{\xi(\xi - \eta)}{\eta} \tilde{\varepsilon}. \quad (106)$$

Finally, solving the term related to (97) provides (26).

APPENDIX C

REPLICA ANALYSIS FOR MATCHED CASE

In the case of matched decoding, the receiver uses the PDF given in (4) for joint detection and decoding and the achievable

rate is the MI defined in (7). One of the terms in the MI can be written

$$-\frac{1}{M} \mathbb{E} \ln p(\mathbf{y} | \mathbf{H}) = f(s) + c, \quad (107)$$

where c is an uninteresting constant that cancels.

The same replica trick we used in Appendix B allows us to write the free energy $f(s)$ as in (65) with

$$\Xi^{(u, M)} = \mathbb{E} \prod_{a=1}^u e^{-(\mathbf{w} + \mathbf{\Delta}_a)^H \mathbf{R}_w^{-1} (\mathbf{w} + \mathbf{\Delta}_a)}, \quad (108)$$

where $\mathbf{\Delta}_a = \mathbf{H}(\mathbf{x}_0 + \mathbf{v}_0) - \mathbf{H}(\mathbf{x}_a + \mathbf{v}_a) = \mathbf{H}\chi_0 - \mathbf{H}\chi_a$ and χ_0, χ_a have the obvious definitions. Here \mathbf{x}_0 is the original transmit vector in (1) and $\{\mathbf{x}_a\}_{a=1}^u$ are replicated data vectors, which are IID drawn according to $p(\mathbf{x})$ when conditioned on $\{\mathbf{x}_0, \mathbf{v}_0, \mathbf{w}, \mathbf{H}\}$. Similarly, \mathbf{v}_0 represents the transmit-side distortion and noise while $\{\mathbf{v}_a\}_{a=1}^u$ are conditionally independent RVs drawn according to the same distribution $g(\cdot | \mathbf{0}; \mathbf{R}_w)$ as \mathbf{v}_0 . The goal is then to assess the normalized free energy (65) by replacing (66) with (108) and $\mathbf{\Sigma} = \mathbf{R}_w$.

For matched decoding, the RS assumption (67)–(70) simplifies as $p = Q \in \mathbb{R}$, $m = q \in \mathbb{R}$ so that $\{\mathbf{\Delta}_a\}_{a=1}^u$ can be written as in (73) with $A = B = Q - q$. Plugging the above into $\Xi^{(u, M)}$ and proceeding as previously yields for any Hermitian and invertible \mathbf{R}_w

$$\Xi^{(u, M)} = (u+1)^{-N} \det(\mathbf{R}_w)^u \mathbb{E}_{\{\chi_a\}} e^{G^{(u)}(Q, q)}, \quad (109)$$

where $G^{(u)}(Q, q) = -u \ln \det \mathbf{\Omega}(Q, q)$ and $\mathbf{\Omega} = \mathbf{\Omega}(Q, q) = \mathbf{R}_w + (Q - q)\mathbf{I}_N$.

The next task is to assess the probability weight of the correlation matrix $\mathbf{Q} \in \mathbb{C}^{(u+1) \times (u+1)}$ whose components are defined in (85). Compared to Appendix B, the only difference is that the RS “Q-matrices” are now of a simpler form since $p = Q$ and $m = q$. This also implies that we may obtain the measure of correlation from Appendix B by setting $\eta = \xi = \tilde{m} = \tilde{q}$. For the per-component MGF we have

$$\phi_m^{(u)}(\tilde{\mathbf{Q}}) = (u+1) \left(\frac{\eta}{\pi} \right)^{-u} \int [\mathbb{E}_{\chi_m} g(z | \chi_m; \eta^{-1})]^{u+1} dz, \quad (110)$$

where $\chi_m = x_m + v_m$ and

$$\eta = \frac{1}{\alpha N} \text{tr}(\mathbf{\Omega}^{-1}). \quad (111)$$

Clearly Q matches now exactly p in (98), while

$$q = \lim_{M \rightarrow \infty} \frac{1}{M} \sum_{m=1}^M \mathbb{E}|x_m + v_m|^2, \quad (112)$$

where

$$\langle \chi_m \rangle = \frac{\mathbb{E}_{\chi_m} \chi_m p(z_m | \chi_m)}{\mathbb{E}_{\chi_m} p(z_m | \chi_m)}. \quad (113)$$

Note that the above estimator is for $\chi_m = x_m + v_m$ and not just for x_m as in the mismatched case (see (102)). The term $\varepsilon = Q - q$ is immediately obtained as given in (49).

For $f(s)$, the equivalent of (106) is

$$\frac{\partial}{\partial u} [(u+1)Q\tilde{Q} + u(u+1)q\tilde{q}] \xrightarrow{u \rightarrow 0} -\eta\varepsilon, \quad (114)$$

and obtained by setting $\xi = \eta$. For the rest of the terms we proceed as before so that defining

$$I(z_m; \chi_m) = -1 - \ln \frac{\pi}{\eta} - \int p(z_m) \ln p(z_m) dz_m, \quad (115)$$

where $p(z) = E_{\chi_m} p(z | \chi_m)$, we have

$$f_{RS} = \frac{1}{\alpha} \left(1 - \frac{1}{N} \ln \det \mathbf{R}_w + \frac{1}{N} \ln \det \mathbf{\Omega} \right) - \eta\varepsilon + \lim_{M \rightarrow \infty} \frac{1}{M} \sum_{m=1}^M I(z_m; \chi_m). \quad (116)$$

The next task is to assess the term

$$\frac{1}{M} E \ln p(\mathbf{y} | \mathbf{x}, \mathbf{H}) = \frac{1}{M} \lim_{M \rightarrow \infty} \frac{\partial}{\partial u} \ln E Z^u(\mathbf{v}, \mathbf{w}, \mathbf{H}) - c, \quad (117)$$

where c is the same constant as in (107) and

$$Z(\mathbf{v}, \mathbf{w}, \mathbf{H}) = E_{\tilde{\mathbf{v}}} e^{-[\mathbf{w} + \mathbf{H}(\mathbf{v} - \tilde{\mathbf{v}})]^H \mathbf{R}_w^{-1} [\mathbf{w} + \mathbf{H}(\mathbf{v} - \tilde{\mathbf{v}})]^H}, \quad (118)$$

since the input \mathbf{x} is known. We obtain the desired result directly from the analysis provided above by letting $\mathbf{\Gamma} \rightarrow \mathbf{0}$; that is, $p(x_m) = \delta(x_m)$. Then $p(z | \chi_m) = g(z_m | v_m; 1/\eta')$ and η' satisfy (50). Similarly,

$$\varepsilon' = Q - q = \lim_{M \rightarrow \infty} \frac{1}{M} \sum_{m=1}^M E |v_m - \langle v_m \rangle|^2, \quad (119)$$

simplifies to (51) since $v_m \sim g(v_m | 0; r_v^m)$. Finally,

$$f'_{RS} = \frac{1}{\alpha} \left(1 - \frac{1}{N} \ln \det \mathbf{R}_w + \frac{1}{N} \ln \det \mathbf{\Omega}' \right) - \eta' \varepsilon' + \lim_{M \rightarrow \infty} \frac{1}{M} \sum_{m=1}^M \ln(1 + \eta' r_v^m). \quad (120)$$

where $\mathbf{\Omega}' = \mathbf{R}_w + \varepsilon' \mathbf{I}_N$ and the MI for matched decoding reads $f_{RS} - f'_{RS}$, as given in (52).

REFERENCES

- [1] D. Tse and P. Viswanath, *Fundamentals of Wireless Communication*. Cambridge University Press, 2005.
- [2] T. C. W. Schenk, P. F. M. Smulders, and E. R. Fledderus, "Performance of MIMO OFDM systems in fading channels with additive TX and RX impairments," in *Proc. 1st Annual IEEE BENELUX/DSP Valley Signal Processing Symposium*, April 2005.
- [3] B. Göransson, S. Grant, E. Larsson, and Z. Feng, "Effect of transmitter and receiver impairments on the performance of MIMO in HSDPA," in *Proc. 9th IEEE Workshop on Signal Processing Advances in Wireless Communications*, July 2008.
- [4] H. Suzuki, T. V. Anh Tran, I. B. Collings, G. Daniels, and M. Hedley, "Transmitter noise effect on the performance of a MIMO-OFDM hardware implementation achieving improved coverage," *IEEE Journal on Selected Areas in Communications*, vol. 26, no. 6, pp. 867–876, August 2008.
- [5] H. Suzuki, I. B. Collings, M. Hedley, and G. Daniels, "Practical performance of MIMO-OFDM-LDPC with low complexity double iterative receiver," in *Proc. 20th IEEE International Symposium on Personal, Indoor and Mobile Radio Communications*, September 2009.
- [6] C. Studer, M. Wenk, and A. Burg, "MIMO transmission with residual transmit-RF impairments," in *Proc. International ITG Workshop on Smart Antennas*, February 2010.
- [7] J. González-Coma, P. M. Castro, and L. Castedo, "Impact of transmit impairments on multiuser MIMO non-linear transceivers," in *Proc. International ITG Workshop on Smart Antennas*, February 2011.
- [8] C. Studer, M. Wenk, and A. Burg, "System-level implications of residual transmit-RF impairments in MIMO systems," in *Proc. 5th European Conference on Antennas and Propagation*, April 2011.
- [9] J. González-Coma, P. M. Castro, and L. Castedo, "Transmit impairments influence on the performance of MIMO receivers and precoders," in *Proc. 11th European Wireless Conference*, April 2011.
- [10] E. Björnson, P. Zetterberg, M. Bengtsson, and B. Ottersten, "Capacity limits and multiplexing gains of MIMO channels with transceiver impairments," *IEEE Communications Letters*, vol. 17, no. 1, pp. 91–94, January 2013.
- [11] X. Zhang, M. Matthaiou, E. Björnson, M. Coldrey, and M. Debbah, "On the MIMO capacity with residual transceiver hardware impairments," in *Proc. IEEE International Conference on Communications*, June 2014, to appear.
- [12] G. Fettweis, M. Löhning, D. Petrovic, M. Windisch, P. Zillmann, and W. Rave, "Dirty RF: A new paradigm," *International Journal of Wireless Information Networks*, vol. 14, no. 2, pp. 133–148, June 2007.
- [13] T. Schenk, *RF Imperfections in High-rate Wireless Systems: Impact and Digital Compensation*. Springer, 2008.
- [14] F. Gregorio, J. Cousseau, S. Werner, T. Riihonen, and R. Wichman, "EVM analysis for broadband OFDM direct-conversion transmitters," *IEEE Transactions on Vehicular Technology*, vol. 62, no. 7, pp. 3443–3451, September 2013.
- [15] N. Merhav, G. Kaplan, A. Lapidoth, and S. Shamai, "On information rates for mismatched decoders," *IEEE Transactions on Information Theory*, vol. 40, no. 6, pp. 1953–1967, November 1994.
- [16] A. Ganti, A. Lapidoth, and I. Telatar, "Mismatched decoding revisited: General alphabets, channels with memory, and the wide-band limit," *IEEE Transactions on Information Theory*, vol. 40, no. 6, pp. 1953–1967, November 2000.
- [17] A. Guillén i Fàbregas, A. Martínez, and G. Caire, "Bit-interleaved coded modulation," *Foundations and Trends in Communications and Information Theory*, vol. 5, no. 1-2, pp. 1–153, 2008.
- [18] W. Zhang, "A general framework for transmission with transceiver distortion and some applications," *IEEE Transactions on Communications*, vol. 60, no. 2, pp. 384–399, February 2012.
- [19] A. T. Asyari and A. Guillén i Fàbregas, "Nearest neighbor decoding in MIMO block-fading channels with imperfect CSIR," *IEEE Transactions on Information Theory*, vol. 58, no. 3, pp. 1483–1517, March 2012.
- [20] H. Nishimori, *Statistical Physics of Spin Glasses and Information Processing*. New York: Oxford University Press, 2001.
- [21] T. Tanaka, "A statistical-mechanics approach to large-system analysis of CDMA multiuser detectors," *IEEE Transactions on Information Theory*, vol. 48, no. 11, pp. 2888–2910, November 2002.
- [22] D. Guo and S. Verdú, "Randomly spread CDMA: Asymptotics via statistical physics," *IEEE Transactions on Information Theory*, vol. 51, no. 6, pp. 1983–2010, June 2005.
- [23] R. R. Müller, "Channel capacity and minimum probability of error in large dual antenna array systems with binary modulation," *IEEE Transactions on Signal Processing*, vol. 51, no. 11, pp. 2821–2828, November 2003.
- [24] C.-K. Wen, K.-K. Wong, and J.-C. Chen, "Spatially correlated MIMO multiple-access systems with macrodiversity: Asymptotic analysis via statistical physics," *IEEE Transactions on Communications*, vol. 55, no. 3, pp. 477–488, March 2007.
- [25] K. Takeuchi, R. R. Müller, M. Vehkaperä, and T. Tanaka, "On an achievable rate of large rayleigh block-fading MIMO channels with no CSI," *IEEE Transactions on Information Theory*, vol. 59, no. 10, pp. 6517–6541, October 2013.
- [26] A. M. Tulino and S. Verdú, "Random matrix theory and wireless communications," *Foundations and Trends in Communications and Information Theory*, vol. 1, no. 1, pp. 1–182, 2004.
- [27] R. Couillet and M. Debbah, *Random Matrix Methods for Wireless Communications*. Cambridge University Press, 2011.
- [28] A. Dembo and O. Zeitouni, *Large Deviations Techniques and Applications*. Springer, 1998.